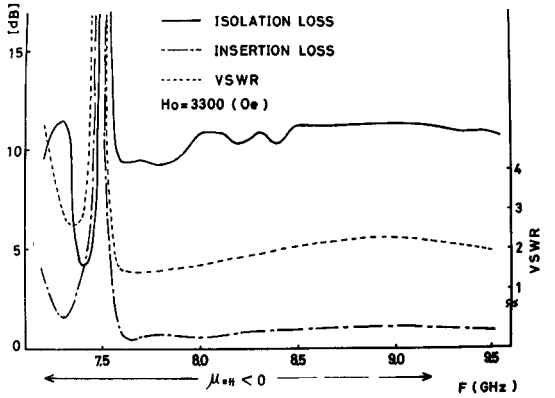

Fig. 12. Computed circulator performance of a triangular circuit at $H_0 = 3300$ Oe for $Z_0 = 50\,\Omega$.

ACKNOWLEDGMENT

The authors wish to thank Prof. T. Okoshi of University of Tokyo for his encouragement.

REFERENCES

[1] T. Okoshi, "The planar circuit," in *Rec. of Professional Groups, IECE of Japan*, Paper SSD68-37/CT68-47, Feb. 17, 1969.
[2] P. P. Civalleri and S. Ridella, "Impedance and admittance matrices of distributed three-layer *N*-ports," *IEEE Trans. Circuit Theory*, vol. CT-17, pp. 392–398, Aug. 1970.
[3] T. Okoshi and T. Miyoshi, "The planar circuit—An approach to microwave integrated circuitry," *IEEE Trans. Microwave Theory Tech.*, vol. MTT-20, pp. 245–252, Apr. 1972.
[4] P. Silvester, "Finite element analysis of planar microwave networks," *IEEE Trans. Microwave Theory Tech.*, vol. MTT-21, pp. 104–108, Feb. 1973.
[5] H. Jui-Pang, T. Anada, and O. Kondo, "Analysis of microwave planar circuits by normal mode method," *Trans. IECE of Japan*, vol. 58-B, pp. 671–678, Dec. 1974.
[6] K. Grüner, "Methods of synthesizing nonuniform waveguides," *IEEE Trans. Microwave Theory Tech.*, vol. MTT-22, pp. 317–322, Mar. 1974.
[7] F. Kato and M. Saito, "Computer-aided desigh of planar circuits," *Trans. IECE of Japan*, vol. J59-A, pp. 47–54, Jan. 1976.
[8] H. Bosma, "On stripline *Y*-circulation at UHF," *IEEE Trans. Microwave Theory Tech.*, vol. MTT-12, pp. 61–72, Jan. 1964.
[9] M. E. Hines, "Reciprocal and nonreciprocal mode of propagation in ferrite stripline and microstrip devices," *IEEE Trans. Microwave Theory Tech.*, vol. MTT-19, pp. 442–451, May 1971.
[10] P. de Santis and F. Pucci, "The edge-guided wave circulator," *IEEE Trans. Microwave Theory Tech.*, vol. MTT-23, pp. 516–519, June 1975.
[11] C. E. Fay and R. L. Comstock, "Operation of the ferrite junction circulator," *IEEE Trans. Microwave Theory Tech.*, vol. MTT-13, pp. 15–27, Jan. 1965.

Energy Analysis for the Amplification Phenomena of Magnetostatic Surface Waves in a YIG-Semiconductor Coupled System

SYOJI YAMADA, NION S. CHANG, MEMBER, IEEE, AND YUKITO MATSUO

***Abstract*—Amplification phenomena of magnetostatic surface waves (MSSW's) in a ferrite–semiconductor system are analyzed in detail for the first time from an energy view point. For the interactions between MSSW's containing a backward branch and carrier streams in a semiconductor, the dispersion relations are given and the energy conservation law is applied to the system. The results in terms of energy quantities are found to be consistent with the solutions of the dispersion equation and well explain the amplifying mechanism macroscopically. We conclude that this kind of interaction is a negative energy dissipation type of instability.**

I. INTRODUCTION

IN SEVERAL YEARS, the investigation of interaction between magnetostatic surface waves (MSSW's) and a carrier stream in semiconductor has been advanced rapidly by many authors [1]–[5]. Recently, we have proposed a general layered structure model consisting of a YIG slab, a semiconductor, dielectrics, and metal plates, and derived a general dispersion equation of the waves. As a result of the analysis, it was concluded that the MSSW's are amplified when the carrier drift velocity v_0 is greater than the phase velocity v_p of MSSW's [6], [7].

In this paper, the interaction between the MSSW mode having a backward branch [8], [9] and a stream of drifting carriers in semiconductor is discussed, including the influence of YIG damping. The ordinary dispersion equation is derived and solved numerically, and then the conservation law of energy appropriate for a dispersive medium is applied to the model of the system. The purpose of our analysis is to show the significance of the De Wames–Wolfram (WW) mode [8] in a practical amplifier design and to interpret the amplifying mechanism, which seems so far not sufficiently clear, in terms of the energy exchange between the waves and the media.

Manuscript received June 7, 1976; revised October 1, 1976.
The authors are with the Institute of Scientific and Industrial Research, Osaka University, Osaka, Japan.

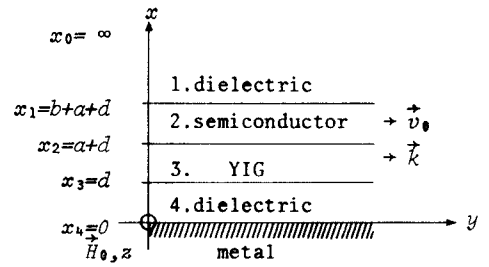

Fig. 1. Analytical model of a layered structure and coordinate system.

II. Dispersion Equation and Energy Method

We first describe briefly the derivation of our dispersion equation. The analytical model of the system is shown in Fig. 1, which is a special case of our general model mentioned earlier [6], [7]. A static biasing magnetic field $\boldsymbol{H}_0$ is applied in the $+z$ direction. The carrier drift velocity $\boldsymbol{v}_0$ in the semiconductor and the MSSW wave vector $\boldsymbol{k}$ are taken to be parallel to the y axis. From Maxwell's equations we can obtain small-signal electric and magnetic field components in four regions under the following assumptions:

1) Two-dimensional analysis: $\partial/\partial z = 0$ and phase factor $\exp i(\omega t - ky)$;
2) Magnetostatic approximations: $\nabla \times H = 0$ in regions 1, 3, and 4;
3) Collision dominance in region 2: $|\omega - kv_0| \ll \nu_c$;
4) The metal plate is assumed to be a perfect conductor [9].

Here ν_c is a collision frequency in the semiconductor. Because of assumptions 1) and 2), only the TE mode (H_x, H_y, E_z) is taken into consideration. Applying boundary conditions to these components, the complex transcendental equation is attained as follows:

$$\exp(2fa) = \frac{A - \tanh fd}{B + \tanh fd} \cdot \frac{B\gamma_s(\gamma_s \tanh \gamma_s b + f) - f(\gamma_s + f \tanh \gamma_s b)}{A\gamma_s(\gamma_s \tanh \gamma_s b + f) + f(\gamma_s + f \tanh \gamma_s b)} \quad (1)$$

$$\left.\begin{aligned} &f = ks \qquad A = \mu_1 + \mu_2 s \qquad B = \mu_1 - \mu_2 s \\ &\gamma_s = \sqrt{k^2 + i\mu_0\sigma(\omega - kv_0)} \qquad s = \pm 1, \quad \text{for } \pm y \text{ propagation} \\ &\mu_1 = 1 + \omega_r\omega_m/(\omega_r^2 - \omega^2) \qquad \mu_2 = \omega\omega_m/(\omega_r^2 - \omega^2)\ \omega_r = \gamma(H_i + i\Delta H/2) \qquad \omega_m = \gamma 4\pi M_s \end{aligned}\right\} \quad (2)$$

where f and γ_s are the wavenumbers of the x direction in YIG and in semiconductor, respectively.

Next we summarize the theory of energy analysis. It is suitable for our aim to adopt the energy method developed on the basis of the so-called "energy conservation law for almost transparent media." It has been established and utilized in unified arguments of wave amplification by Musha and Agu [10], [11].

The conservation law can be derived from Maxwell's equations in the Minkowski formulation, provided that the medium is almost transparent for the waves. In other words, it is assumed that $|\varepsilon_r| \gg |\varepsilon_i|$ and $|\mu_r| \gg |\mu_i|$, where $\varepsilon = \varepsilon_r + i\varepsilon_i$ is the effective permittivity and $\mu = \mu_r + i\mu_i$ is the effective permeability of the medium, in which the motions of electrons or spins are included. The conservation law is conveniently written for an isotropic medium as follows:

TABLE I
Effective Permittivity and Permeability (Tensor) of Four Regions in Fig. 1

region	ε	μ
1,4	ε_0	μ_0
2	$\varepsilon_0\varepsilon_s - \sigma k_i v_0/\omega^2$ $-i\sigma(\omega - k_r v_0)/\omega^2$	μ_0
3	$\varepsilon_0\varepsilon_f$	$\mu_0 \begin{bmatrix} \mu_1 & i\mu_2 & 0 \\ -i\mu_2 & \mu_1 & 0 \\ 0 & 0 & 1 \end{bmatrix}$

where ε_s and ε_f are dielectric constant of semiconductor and YIG respectively. σ is a conductivity.

$$\partial w/\partial t + \nabla \cdot \boldsymbol{s} + q = 0 \quad (3)$$

$$w = \tfrac{1}{2}\{(\partial\omega\varepsilon_r/\partial\omega)\langle \boldsymbol{E}^2\rangle + (\partial\omega\mu_r/\partial\omega)\langle \boldsymbol{H}^2\rangle\} \quad (4)$$

$$\boldsymbol{s} = \langle \boldsymbol{E} \times \boldsymbol{H}\rangle - \tfrac{1}{2}\{(\partial\omega\varepsilon_r/\partial \boldsymbol{k})\langle \boldsymbol{E}^2\rangle + (\partial\omega\mu_r/\partial \boldsymbol{k})\langle \boldsymbol{H}^2\rangle\} \quad (5)$$

$$q = -\omega(\varepsilon_i\langle \boldsymbol{E}^2\rangle + \mu_i\langle \boldsymbol{H}^2\rangle) \quad (6)$$

where ω and $\boldsymbol{k}$ are real, and the symbol $\langle\ \rangle$ indicates an average over a period. The above three quantities, i.e., the energy density of the wave w, the energy flow density $\boldsymbol{s}$, and the energy dissipation density q are known to be related to such characterizing quantities as the attenuation constant $k_i = \operatorname{Im} k$ and the group velocity $v_g = \partial\omega/\partial k_r$ by the following equations:

$$k_i = -q/2s_{\parallel} \quad (7)$$

$$v_g = s_{\parallel}/w \quad (8)$$

where subscript $\parallel$ refers to the component of $\boldsymbol{s}$ parallel to $\boldsymbol{k}$. Therefore, if we wish to obtain information related to the macroscopic structure of the wave instability, the variations of w, $\boldsymbol{s}$, and q must be studied in detail.

In order to apply this method to our layered structure model, it is necessary to modify these energy quantities, since (3)–(6) are appropriate only for a unit cell in an infinite medium. The application has been done by the following three step procedures.

1) In four regions of Fig. 1, each w, $\boldsymbol{s}$, and q may be found from the TE mode components and the effective material constants (or tensor) of each medium given in Table I. It is noted that in the YIG region, another form of (4)–(6) must be used replacing $\mu = \mu_r + i\mu_i$ with $\tilde{\mu} = \tilde{\mu}^h + \tilde{\mu}^a$, where $\tilde{\mu}$ is an effective permeability tensor, and the superscripts h and a denote the Hermitian and anti-Hermitian part of the tensor, respectively [11].

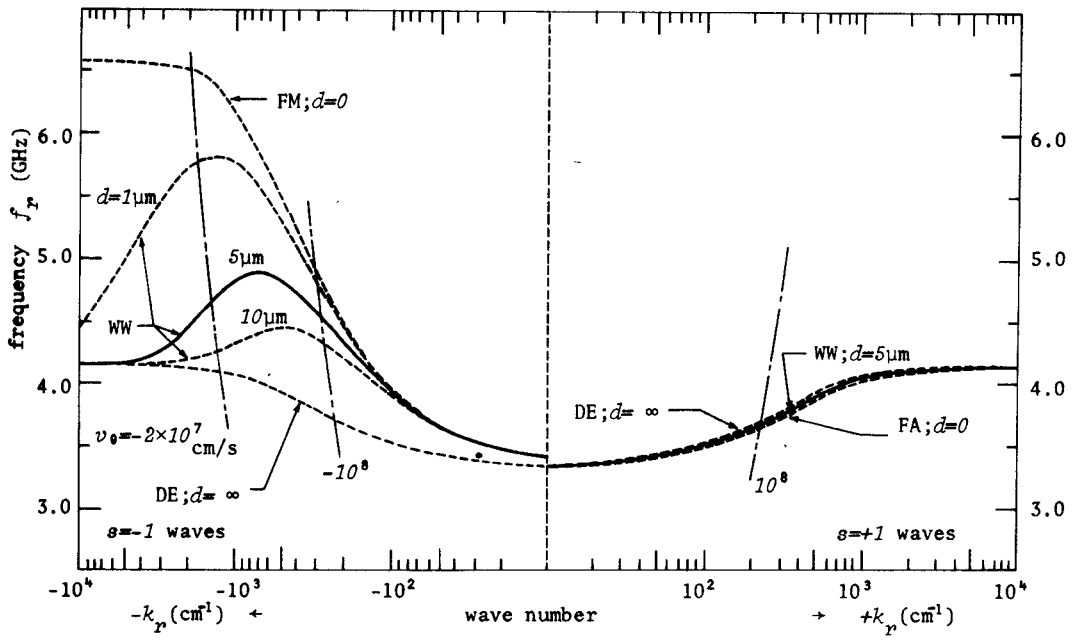

Fig. 2. Brillouin diagram of MSSW $s = \pm 1$ waves in a YIG- semiconductor composite system. ——— the modes we deal with here. ------- other modes when $d \neq 5$ μm. ——·—— $\omega/k_r = v_0$. Thicknesses and parameters used are as follows: $b = 1$ μm, $a = 10$ μm, and $d = 5$ μm for semiconductor, YIG, and dielectric, respectively. Internal magnetic field $H_i = 600$ Oe ($=H_0$ in our geometry) and the saturation magnetization of YIG $4\pi M_s = 1750$ G. The carrier density $n_0 = 10^{15}/\text{cm}^3$ and the mobility $\mu_m = 2.2 \times 10^5$ cm^2/V·s in semiconductor.

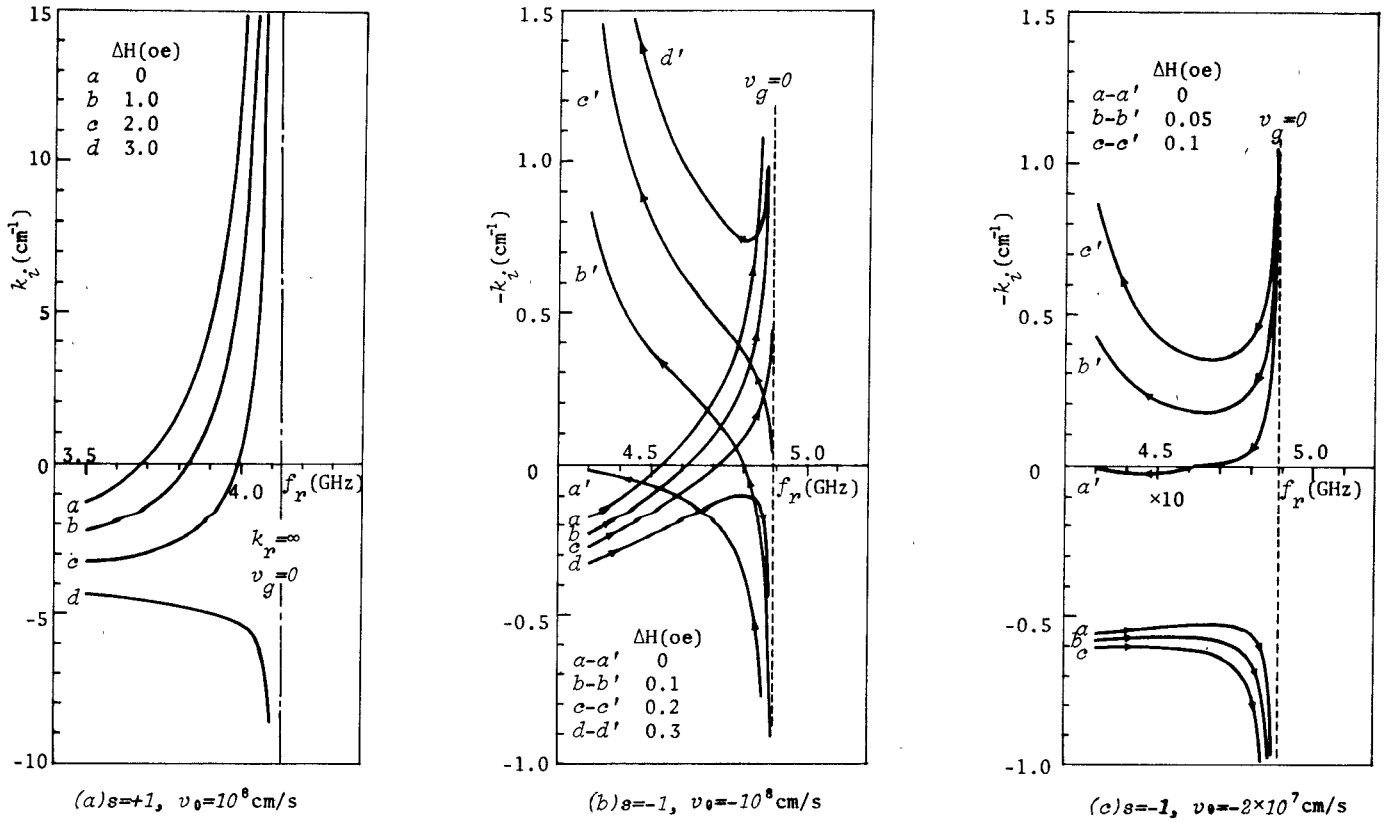

Fig. 3. Attenuation constant k_i against operation frequency f_r for three interaction cases. Note that the ordinates of (b) and (c) are inverted to that of (a). Arrows on the curves in (b) and (c) mean as follows: —→— forward branch, —←— backward branch. Therefore, for example, $a - a'$ is a set of these forward–backward branches. The positive portion of k_i in (c) is ten times magnified.

2) Integrating these quantities from zero to infinity along the x axis, we redefine equivalent energy quantities, namely W, S, and Q. For example, S is

$$S_y \equiv \int_0^\infty s_y \, dx = \sum_{i=1}^{4} S_{yi} \tag{9}$$

$$S_{yi} = \int_{x_i}^{x_{i-1}} s_{yi} \, dx, \qquad i = 1 \sim 4 \tag{10}$$

$$\bar{S}_{xi} \equiv \int_{x_i}^{x_{i-1}} s_{xi} \, dx/(x_{i-1} - x_i) \tag{11}$$

where x_is are indicated in Fig. 1. W and Q are also redefined as S_y. As is seen in (9) and (10), W, S_y, and Q are the sum of four parts formally. However, the following significant features of Q are easily understood from (6) and Table I.

a) Q has really only two parts in itself, i.e., $Q = Q_2$ (semiconductor) + Q_3(YIG).
b) Q_2 is proportional to $(v_0 - v_p)$ and therefore $Q_2(v_0 = v_p) = 0$.
c) Q_3 is a function of FMR linewidth ΔH and $Q_3(\Delta H = 0) = 0$.

3) The numerical calculations are carried out, substituting frequencies and the solutions of (1) in W, S, and Q. Finally, the accuracy of these calculated values is examined by comparing the two quantities

$$k_{i,\text{macro}} = -Q/2S_y = -(Q_2 + Q_3)/2S_y \tag{12}$$

$$v_{g,\text{macro}} = S_y/W \tag{13}$$

with the results of the dispersion analysis, that is, $k_i' = \text{Im}\, k$ and $v_g' = \Delta\omega/\Delta k_r$, respectively. Equations (12) and (13) are also derived from (7) and (8).

III. Numerical Results and Discussions

The parameters assumed in our calculations are as follows: Thicknesses are $b = 1$ μm (semiconductor), $a = 10$ μm (YIG), and $d = 5$ μm (dielectric). The internal magnetic field $H_i = 600$ Oe ($= H_0$ in our geometry) and the saturation magnetization of YIG $4\pi M_s = 1750$ G. The carrier density n_0 and the mobility μ_m of the semiconductor are $10^{15}/\text{cm}^3$ and 2.2×10^5 cm^2/V · s, respectively.

Firstly, since we are interested in convective-type instability, we have solved (1) in the form of a complex wave number $k = k_r + ik_i$ for a given frequency $f_r = \omega/2\pi$. Fig. 2 shows the Brillouin diagrams of coupled MSSW's. Solid lines are the case we treat here and correspond to $d = 5$ μm. The dotted curves obtained when $d \neq 5$ μm are shown for comparison. As is well known, d has an important effect particularly on the characteristics of $s = -1$ waves. It is customary to refer to MSSW modes as ferrite–air and ferrite–metal modes if $d = 0$ [12], WW modes if $d \neq 0$ [9], and Damon–Eshbach modes if $d \to \infty$ [13]. Among these modes, only the WW has backward branches. Though our model is complicated, it is more interesting in this sense. Further, the curves $\omega/k_r = v_0 = \pm 10^8$, -2×10^7 cm/s are inserted in Fig. 2 by chain dotted lines. We consider

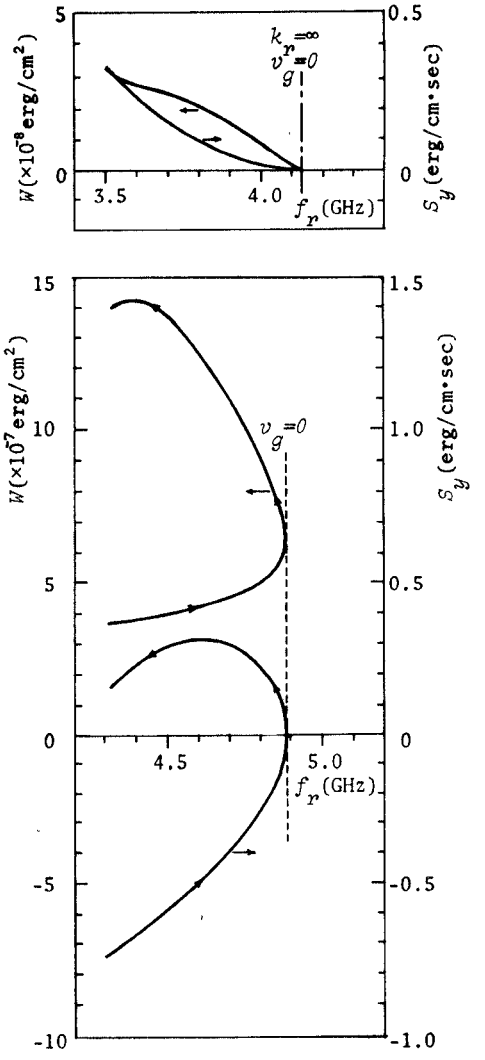

Fig. 4. Energy W and energy flow in y direction S_y of $s = \pm 1$ waves versus frequency f_r. It is noted in Figs 4 and 5 that the energy quantities are plotted as relative values obtained when the amplitude of electric field in semiconductor is normalized. Arrows in (b) have the same meanings as in Fig. 3. (a) $s = +1$. (b) $s = -1$.

here three interaction cases as follows:

1) $s = +1$ and $v_0 = +10^8$ cm/s;
2) $s = -1$ and $v_0 = -10^8$ cm/s;
3) $s = -1$ and $v_0 = -2 \times 10^7$ cm/s.

The attenuation constants in each case are plotted as a function of frequency in Fig. 3(a)–(c) with ΔH as a parameter. Similar to the $\omega - k_r$ diagram, $s = -1$ waves have two k_i values for a frequency f_r and so the two branches of the waves are made distinguishable with arrows on the curves which indicate the direction in which k_r increases. This representation is employed also in Figs. 4(b) and 5(b), (c). The criteria for the convective instability are $k_i > 0$ for $s = +1$ and $s = -1$ backward branch, and $k_i < 0$ for $s = -1$ forward branch [14]. Applying these conditions to Fig. 3(a)–(c), we find that the wave amplification occurs only in the frequency range such that $v_0 > v_p$ in all cases. The bandwidth with gain, however, decreases and soon disappears with increasing ΔH. It is also found in the figures that the interaction strength which is reflected in the magni-

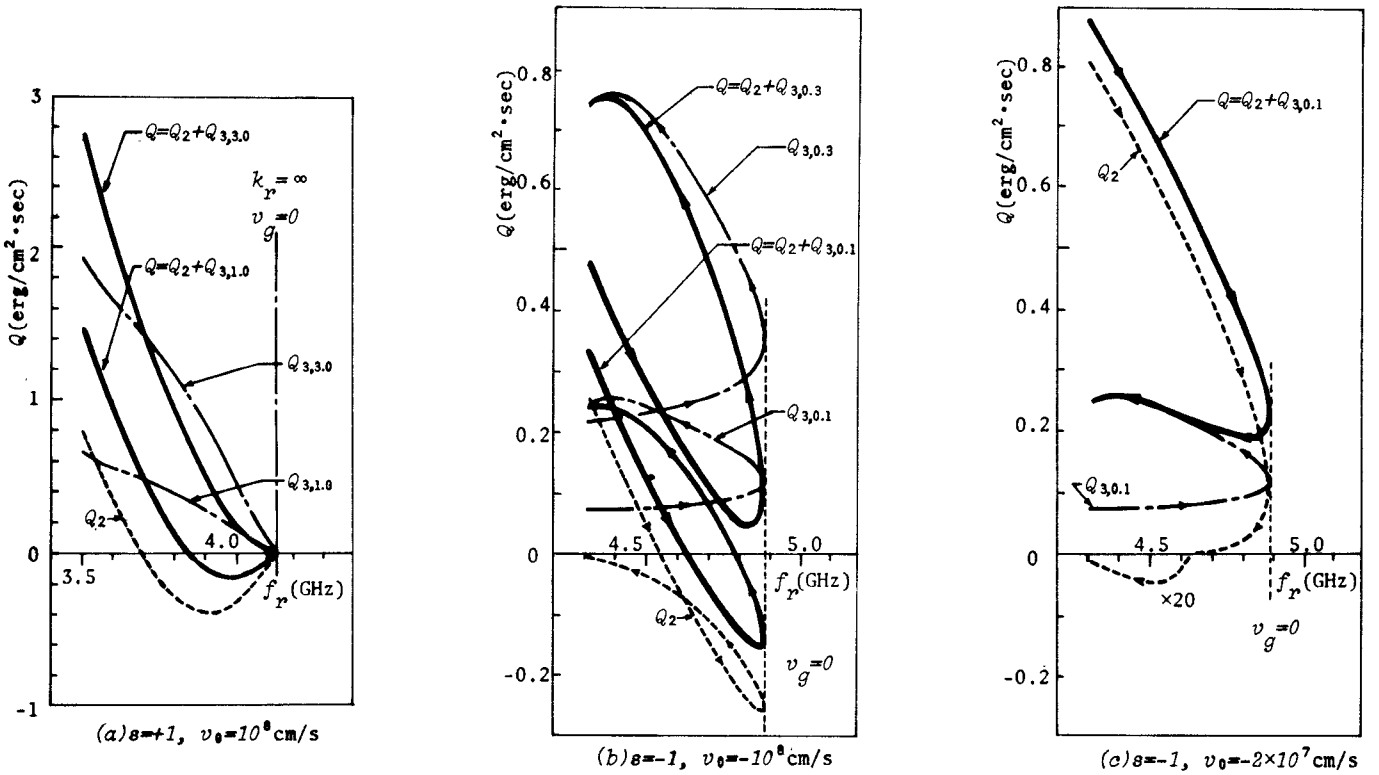

Fig. 5 Energy dissipation Q and its two elements Q_2 and Q_3 versus frequency f_r for the three interaction cases. ——— $Q = Q_2 + Q_3$. --------- Q_2. ——— Q_3. $Q_{3,\alpha}$ means $Q_3(\Delta H = \alpha$ Oe). Arrows in (b) and (c) also have the same meanings as in Fig. 3. The negative Q_2 in (c) is illustrated in a twenty-times-multiplied scale.

tude of $|k_i|$ and hence the sensitivity against ΔH of $s = +1$ is about ten times greater than that of $s = -1$. The origin of the difference should be attributed to the unique features of MSSW's that $s = +1$ wave propagates on the semiconductor side of the YIG plate and $s = -1$ wave on the opposite in Fig. 1. But it should be pointed out that the wave $s = -1$ is practically important, because the backward region of the wave can interact with slower carrier flow as shown in case 3). To increase the gain [ten times magnified in Fig. 3(c)], one has only to insert the semiconductor between YIG and the dielectric layer in Fig. 1.

Secondly, the results of energy calculations are illustrated in the next two figures and Table II. Fig. 4(a), (b) shows energy W and energy flow in y direction S_y versus f_r for $s = \pm 1$ waves. In Fig. 5(a)–(c), the energy dissipation Q and its two elements, i.e., Q_2 and Q_3, are plotted versus f_r for the former three interaction cases. From these results we estimate $k_{i,\text{macro}}$ and $v_{g,\text{macro}}$ by substituting W, S_y, and Q into (12) and (13). We find that the values of the two quantities agree well with k_i' and v_g', respectively, obtained in Figs. 2 and 3. This fact signifies the consistency of both results.

To understand the rather complex results of Figs. 4 and 5, we first pay attention to the variations of the signs of W, S_y, and Q. Then we write down Table II from the figures for three interaction cases together with that of some related parameters, if $\Delta H = 0$. The table clearly shows that whenever Q is negative, the instability occurs regardless of the directions of S_y which coincides with that of v_g, and that W is always positive. This situation is not changed much if

TABLE II
VARIATIONS OF SIGNS OF W, S_y, AND $Q(=Q_2)$ ALONG WITH THAT OF SOME IMPORTANT QUANTITIES

case	(a)		(b)			(c)		
v_0	10^8cm/s		-10^8cm/s			-2×10^7cm/s		
MSSW	$s=+1$		$s=-1$			$s=-1$		
quantity	forward $v_0=v_p$		forward $v_0=v_p$		backward	forward	backward $v_0=v_p$	
$v_p=\omega/k_r$	+	+	-	-	-	-	-	-
v_0-v_p	-	+	-	+	+	-	-	+
W	+	+	+	+	+	+	+	+
S_y	+	+	-	-	+	-	+	+
$Q=Q_2$	+	-	+	-	-	+	+	-
$v_g=S_y/W$	+	+	-	-	+	-	+	+
$k_i=-Q/2S_y$	-	+*	+	-*	+*	+	-	+*

* indicates amplifying.

Note: For simplicity, the $\Delta H = 0$ case is tabulated.

$\Delta H \neq 0$. But in the latter case, the negative Q_2 is reduced by the element Q_3 which is always positive as seen in Fig. 5. The decrease of negative Q results in the narrower bandwidth with gain in Fig. 3. Thus in our macroscopic descriptions of the system, the instability of MSSW's is subject to the condition that energy dissipation is negative.

These circumstances are explained physically as follows: The carrier stream in semiconductor changes from an energy dissipator ($Q_2 > 0$) to an energy radiator ($Q_2 < 0$)

for the MSSW as v_0 becomes greater than v_p. The energy from the semiconductor is received—wholly ($Q_3 = 0$) or partly ($Q_3 < |Q_2|$)—by the MSSW and, consequently, the amplitude of the waves becomes larger. But if YIG damping is so great that $Q_3 > |Q_2|$, the radiated energy is all dissipated in YIG loss and does not contribute to the amplification.

IV. Conclusion

In the preceding section, the amplifying characteristics of the MSSW WW mode caused by a carrier flow in semiconductor have been investigated by using the dispersion equation and the energy conservation law for almost transparent media. It is pointed out that the WW mode is favorable to amplification, since it has a backward branch interacting with a slower drifting carrier. One of the important results of our energy analysis is that the MSSW instability occurs only when the energy dissipation of the media is negative for the waves. If this result is combined with Schlömann's microscopic and qualitative work [15], one may easily appreciate the amplifying mechanism of this type physically and construct a total picture of the system.

References

[1] N. S. Chang and Y. Matsuo, "Possibility of utilizing the coupling between a backward wave in YIG and waves associated with drift carrier stream in semiconductor," *Proc. IEEE*, vol. 56, pp. 765–766, Apr. 1968.
[2] A. V. Vashkovskii, V. I. Zubkov, V. N. Kildshev, and B. A. Murmuzhev, "Interaction of surface magnetostatic waves with carrier on a ferrite-semiconductor interface," *Sov. Phys. JETP Letters*, vol. 16, pp. 4–7, 1972.
[3] M. Szustakowski and B. Wecki, "Amplification of a magnetostatic surface wave in the YIG-Ge hybrid system," *Proc. of Vibration Problems*, vol. 14, pp. 155–163, 1973.
[4] V. P. Lukomskii and Yu. A. Tsvirko, "Amplification of magnetostatic waves in a ferromagnetic film due to the drift current of carriers," *Sov. Phys. Solid State*, vol. 15, pp. 492–495, 1973.
[5] M. Masuda, N. S. Chang, and Y. Matsuo, "Magnetostatic surface waves in ferrite slabs adjacent to semiconductor," *IEEE Trans. Microwave Theory Tech.*, vol. MTT-22, pp. 132–135, Feb. 1974.
[6] N. S. Chang, S. Yamada, and Y. Matsuo, "Characteristics of magnetostatic surface-wave propagation in a layered structure consisting of metals, dielectrics, a semiconductor and Y.I.G.," *Electron. Lett.*, vol. 11, pp. 83–85, Feb. 1975.
[7] ——, "Amplification of magnetostatic surface waves in a layered structure consisting of metals, dielectrics, a semiconductor and Y.I.G.," *J. Appl. Phys.*, vol. 47, pp. 385–387, Jan. 1976.
[8] R. E. De Wames and T. J. Wolfram, "Characteristics of magnetostatic surface waves for a metalized ferrite slab," *J. Appl. Phys.*, vol. 41, pp. 5243–5246, Dec. 1970.
[9] H. Van De Vraat, "Influence of metal plate on surface magnetostatic modes of magnet slab," *Electron. Lett.*, vol. 6, pp. 601–602, Sept. 1970.
[10] T. Musha, "Wave amplification in moving dispersive media," *IECE Japan*, vol. 51, pp. 614–620 (Part I), May 1968, pp. 760–765 (Part II), June 1968.
[11] T. Musha and M. Agu, "Energy and power flow of a moving dispersive media," *J. Phys. Soc. Japan*, vol. 26, pp. 541–549, Feb. 1969.
[12] S. R. Seshadri, "Surface magnetostatic modes of a ferrite slab," *Proc. IEEE*, vol. 58, pp. 506–507, Mar. 1970.
[13] R. W. Damon and J. R. Eshbach, "Magnetostatic modes of a ferromagnet slab," *J. Phys. Chem. Solid*, vol. 118, pp. 308–320, July 1960.
[14] R. J. Briggs, *Electron Stream Interaction with Plasma*. MIT Press, 1964.
[15] E. Schlömann, "Amplification of magnetostatic surface waves by interaction with drifting charge carriers in crossed electric and magnetic fields," *J. Appl. Phys.*, vol. 40, pp. 1422–1424. Mar. 1969.

On Microwave-Induced Hearing Sensation

JAMES C. LIN, MEMBER, IEEE

***Abstract*—When a human subject is exposed to pulsed microwave radiation, an audible sound occurs which appears to originate from within or immediately behind the head. Laboratory studies have also indicated that evoked auditory activities may be recorded from cats, chinchillas, and guinea pigs. Using a spherical model of the head, this paper analyzes a process by which microwave energy may cause the observed effect. The problem is formulated in terms of thermoelasticity theory in which the absorbed microwave energy represents the volume heat source which depends on both space and time. The inhomogeneous thermoelastic motion equation is solved for the acoustic wave parameters under stress-free surface conditions using boundary value technique and Duhamel's theorem. Numerical results show that the predicted frequencies of vibration and threshold pressure amplitude agree reasonably well with experimental findings.**

Manuscript received July 12, 1976; revised October 5, 1976. This work was supported in part by the National Science Foundation under Grant ENG 75-15227.

The author is with the Department of Electrical and Computer Engineering, Wayne State University, Detroit, MI 48202.

I. Introduction

IT HAS BEEN demonstrated that sound can be generated in laboratory animals by the absorption of microwave energy in the head [1]–[3]. These reports indicate that auditory activities may be evoked by irradiating the heads of cats, chinchillas, and guinea pigs with pulsed microwave energy [1], [4]–[6]. Responses elicited in cats by both conventional acoustic stimuli and by pulsed microwaves disappear following destruction of the round window of the cochlea [4], and following death [3]. This suggests that microwave-induced audition is transduced by a mechanism similar to that responsible for conventional acoustic reception, and that the primary site of interaction resides peripherally with respect to the cochlea. More recently [6], sonic oscillations at 50 kHz have been recorded from the round window of guinea pigs during irradiation by pulsed